Desalination and Water Treatment
www.deswater.com

doi: 10.1080/19443994.2015.1108234

57 (2016) 20350–20367
September

Taylor & Francis
Taylor & Francis Group

Removal of copper(II) ions from synthetic electroplating rinse water using polyethyleneimine modified ion-exchange resin

Meyyappan Revathi[a], Chiya Ahmed Basha[b], Manickam Velan[a,*]

[a]*Department of Chemical Engineering, AC College of Technology, Anna University, Chennai 600 025, India, email: mrev80@gmail.com (M. Revathi), Tel. +044 2235 9117, ext. 7122; email: velan@annauniv.edu (M. Velan)*
[b]*Pollution Control Division, Central Electrochemical Research Institute, Karaikudi 630 006, Tamil Nadu, India, email: cabasha@gmail.com*

Received 28 December 2014; Accepted 10 October 2015

ABSTRACT

Removal of copper ions (Cu(II)) from synthetic electroplating rinse water (SEPRW) by using modified ion-exchange resin was investigated. Modification of the cationic exchange resin was carried out by impregnating polyethyleneimine (PEI). Impregnation was confirmed by scanning electron microscopy–energy dispersive X-ray analysis and Fourier transform infrared spectroscopy analyses. Batch studies were conducted to optimize the various experimental parameters such as contact time, pH, and dosage. The influence of other process parameters including the presence of chelating agent ethylene diamine tetra acetic acid (EDTA) and co-ions were examined. A maximum adsorption capacity (Q_{max}) of 667.5 mg g^{-1} was observed at the optimum conditions. Cu(II) removal efficiency of the polyethyleneimine modified ion-exchange resin (PMR) was compared with the unmodified resin (UMR). After the impregnation of PEI, adsorption capacity of the resin varied and the removal rate of Cu(II) removal became fast. Continuous column experiments were conducted in a glass column of desired dimensions. The maximum Cu(II) uptake was obtained at the bed height of 1.65 dm and flow rate of 0.015 L min^{-1}. The breakeven point of the column was obtained after the treatment of 19.5 L of SEPRW. Adam–Bohart and Yoon Nelson models were applied to the column data and desorption studies were conducted in batch mode using hydrochloric acid (HCl), nitric acid (HNO_3) and sulphuric acid (H_2SO_4) as eluant.

Keywords: Polyethyleneimine modified ion-exchange resin; Copper; Electroplating rinse water; Batch study; Column study

1. Introduction

Metal finishing industrial processes emit considerable volume of residual water contaminated with heavy metals such as copper, cadmium, zinc, nickel and chromium. These metal ions cause a serious problem to the environment and public health when they contaminate superficial and groundwater. The heavy metal ions are not biodegradable and tend to accumulate in living organisms leading to several types of diseases and disturbances [1]. Copper is widely employed in most of the industrial processes. Excessive levels of copper may damage liver and kidney, and may be responsible for anaemia,

*Corresponding author.

immunotoxicity and developmental toxicity. The co-carcinogenic character of copper is also implicated in stomach and lung cancers [2]. Electroplating and printed circuit board industries are the major sources of copper pollution. The rinse water usually employed after plating process having the metal ions is known to be the major source for waste pollution and the loss of useful chemicals. Removal of copper ions (Cu(II)) from aqueous systems is therefore an important area of study. This can be achieved by transfer of the metal ions from the aqueous phase to a solid phase by the process of adsorption. The solid phase should have strong affinity for the target metal ions, binding them irreversibly under ambient conditions, and simultaneously possessing the ability to release the same under different conditions such that it can be regenerated for further use [3]. Several different solid phases have been found useful in the removal of Cu(II) from solution including bacteria [4], algae [5], yeast [6], fungi [7], cabbage and cauliflower wastes [8], Algerian bentonite [9], saw dust [10], tire rubber [11], tea leaves [12], pomegranate peel [13] and zeolite [14], etc.

In recent years, the greater attention was focused on the development of nanoparticles and their application for the removal of heavy metal ions from the wastewater. Different forms of iron oxide nanoparticles like maghemite [15], goethite and haematite [16] were prepared and experimented for the removal of Cu(II) ions from the aqueous solutions. The surface of the Fe_3O_4 magnetic nanoparticles were modified with chelating diamines [17], amino propyl triethoxy silane (APTES) and glutaraldehyde (GA) [18], their Cu(II) adsorption behaviour from aqueous solution was determined. Thiol functionalized super paramagnetic nanoparticles [19], magnetic chitosan nanocomposites [20] were also tried as sorbents for heavy metal removal.

Rengaraj et al. studied and found that ion-exchange resins Amberjet 254H and Ambersep 1500H as good adsorbents for the removal of Cu(II) ions [21]. Verbych et al. experimented and stated that some universal cation exchangers were found as good adsorbents for the removal of Cu(II) and Ni(II) ions [22]. Removal of Ni(II) and Zn(II) ions were studied using Dowex HCR S/S resins by Alyuz and Veli [23].

The introduction of nanoparticle into the resin matrix for the improved removal of heavy metals becomes more interesting topic nowadays. Several studies were conducted to improve the adsorption capacity of ion-exchange resin and the selectivity of trace metal ions. The porous resin impregnated with nanoparticles offered many advantages over the other sorbents, due to characteristics of the solid phase. These advantages include, selectivity, mechanical stability, size controllable nanoparticles, easy regeneration for multiple sorption–desorption cycles and good reproducibility of the sorption characteristics. The sorption of precious metals on a macro porous resin impregnated with magnetite nanoparticles [24], Amberlite XAD-4 modified with nonionic surfactant—trioctylamine (TOA) [25], D001 impregnated with PEI [26], Amberlite-200 composite with PEI, TBAI, TMAH solutions [27] have been reported.

Among these polyethyleneimine (PEI) is a polymeric nanocluster used for a wide variety of applications. These include electrochemical biosensors, cell flocculating agents, permeabilization of bacterial cell walls, retention of nicotinamide adenine dinucleotide (NADH) in membrane reactors, adsorption of biomass and microencapsulation of silicone oils. The immobilization of PEI in a suitable matrix can provide an attractive alternative to membrane processes. Chanda and Rempel applied PEI-containing granular sorbents for the selective removal of Cr(III) in a mixture of Cr(III), Cu(II), Ni(II) and Fe(III). This sorbent was found to be superior to the commercial resin Chelex-100 [28].

In this present study, attempts were made to prepare a PEI-impregnated Ceralite IR 120 ion-exchange resin using nonhazardous PEI solution for the selective separation of Cu(II) from synthetic electroplating rinse water (SEPRW) solutions. The presence of PEI in the resin was characterized by scanning electron microscopy–energy dispersive X-ray analysis (SEM-EDX), Fourier transform infrared spectroscopy (FTIR) measurements. The effect of various experimental parameters on Cu(II) removal from SEPRW by PMR was studied with the help of batch shaking experiments. In addition, the presence of chelating agent EDTA and co-existing cation on metal removal efficiency were examined. Experimental results obtained with the optimum conditions were used to fit isotherm models, namely Langmuir and Freundlich isotherms. Experimental data were fitted with pseudo-first- and second-order kinetic models. Column studies were performed in batch recirculation mode by varying initial concentration of Cu(II) ions, the flow rate of inlet metal solutions and bed height. The continuous breakthrough analysis was carried out at the highest bed height, optimum flow rate for an initial Cu(II) concentration of 500 mg L^{-1}. The dynamic behaviour of the column was analysed by Adams–Bohart, Yoon and Nelson and bed depth service time (BDST) models. Desorption of the loaded heavy metal ions from the resin column was studied by using sulphuric acid as an eluant. The results obtained with the PMR were compared with data reported in the literature with the unmodified resin, UMR [29].

2. Materials and methods

All the reagents and chemicals used were of analytical grade. SEPRW samples having different Cu(II) ions concentration (Cu(II) = 200, 300,400 and 500 mg L^{-1}) were prepared by diluting the copper electrolytic bath of the following composition: 200 g L^{-1} of $CuSO_4$, 75 g L^{-1} of H_2SO_4. Table 1 shows the physical properties of cation-exchange resin Ceralite IR 120. The resin is a strongly acidic cationic exchange resin. It has fairy good capacity and unusual stability at elevated temperatures. All the solutions were made with double distilled water. The Ceralite IR120 cation-exchange resin was purchased from CDH, New Delhi. Before using them, the resin was soaked in double distilled water for 12 h and then they were also washed several times with double distilled water. Polyethyleneimine (PEI) is an Aldrich product (M_n—60,000, M_w—7, 50,000, 50% aqueous solution) purchased from Sigma Aldrich Chem. Co. (USA).

2.1. Modification of Ceralite IR 120

Five grams of resin was immersed in 0.02 L of 0.05 Molar (M) (2/5 water, 3/5 alcohol) PEI solution and agitated constantly using a glass agitator connected with an electric driving force for 7 d at constant room temperature (32˚C) [30]. The hydrophobic property of the resin increased after introducing these amorphous branched structure with a distribution of primary, secondary and tertiary amino groups in the ratio 1:2:1 [31], adsorbed and/or ion exchanged with H^+ counter-ion on the surface. Therefore, the resin obtained had the following principal characteristics:

Table 1
Physical properties of cation exchange resin Ceralite IR 120

Parameter	Ceralite IR 120
Manufacturer	CDH, New Delhi
Ionic group	H^+ strongly cation exchange resin
Particle size	0.45–0.6 (effective size)mm
Physical form	Yellow brown spherical beads
Density	770 kg m^{-3}
Exchange capacity (fresh)	4.5 mequiv. g^{-1}
Moisture content	45–50 wt.%
Maximum temperature	120˚C
pH range	0–14
Cross linking	8% DVB
Porosity	0.42
Nominal diameter	0.5 mm

UMR has a low distribution coefficient. PMR has a preferential selectivity towards heavy metals and particularly for the Cu(II). However, the PEI molecules would desorb from the resin surface during subsequent sorption and regeneration processes. To fix the PEI onto the surface permanently, the modified ion-exchange resin was soaked in 1% glutaraldehyde in isoproponal as the cross linking agent for 20 min [32]. PMR was washed with distilled water and soaked in 0.5 Normal (N) NaOH solutions for 3 h to change them to Na^+ form (Fig. 1).

2.1.1. Characterization of modified resin

The change in surface morphology of the parent resin was analysed by SEM–EDX. The magnified image of the surface of the ion-exchange resin was captured in scanning electron microscopy (SEM) Hitachi S-3400N Magnification 5× 300,000× type of instrument. The FTIR Spectra of UMR, PMR were taken in Perkin Elmer-Spectrum RX1 FTIR.

2.2. Batch adsorption studies

The adsorption capability of PMR and UMR towards Cu(II) ions at room temperature (35˚C) was investigated using SEPRW having copper concentration of 200 mg L^{-1}. The extent of Cu(II) ion removal was calculated from the residual concentration of sorbate in equilibrated solution. The effect of pH of the medium on the adsorption process was studied at the pH values where no chemical precipitation of Cu $(OH)_2$ occurs (i.e. 2–8). The optimum pH value obtained from this study was fixed for further experiments. The minimum contact time, adsorbent dosage required for maximum Cu(II) uptake was studied by varying the contact time from 1 to 60 min and adsorbent dosage from 0.125 to 2.0 g L^{-1}. In addition, the influence of other experimental parameters such as presence of additive (EDTA), co-ions (Ni, Zn) on the adsorption process were also studied. The concentration of Cu(II) present in the rinse water samples was determined using Varian model Spectraa 220 Atomic Absorption spectrophotometer (AAS). Cu(II) uptake (mg g^{-1} resin) at equilibrium conditions was calculated from:

$$q_e = \frac{(C_0 - C_e)V}{m} \quad (1)$$

where V is the volume of sample in litres. C_0 and C_e are concentration of Cu(II) in mg L^{-1} and W is amount of resin in grams.

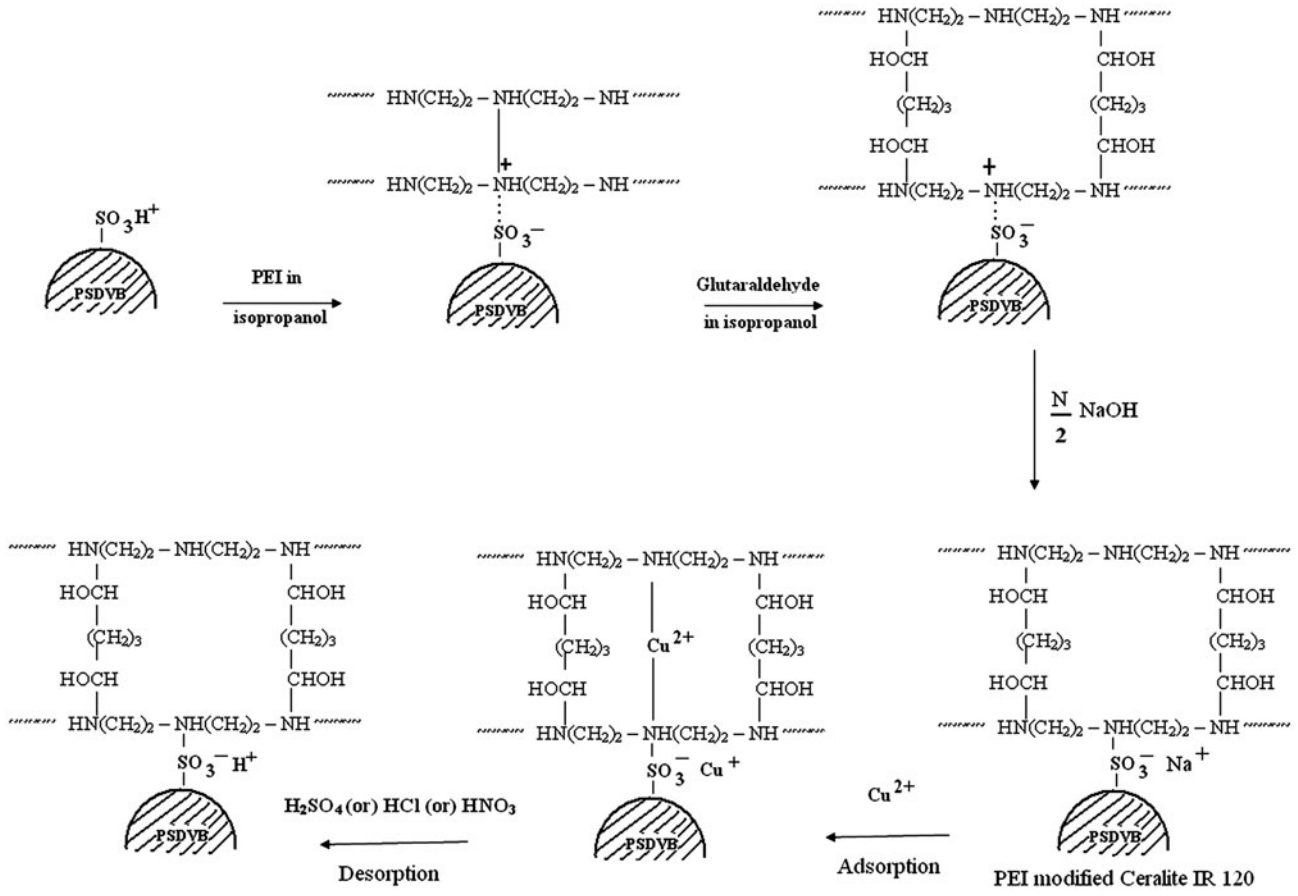

Fig. 1. Schematic diagram of preparation of PEI modified resin (PMR).

2.2.1. Regeneration of modified Ceralite IR 120

An amount of 0.1 g of Cu(II) saturated PMR was immersed in 0.1 L of different acid solutions (0.5 M HNO_3, 0.5 M HCl and 0.5 M H_2SO_4), and the systems were agitated for 2 h, then filtered. The filtrate was analysed for Cu(II) by AAS and the percentage of elution (E %) was calculated from the equation:

$$E\ \% = \frac{(M^{n+})_{\text{eluted}}}{(M^{n+})_{\text{fixed}}} \times 100 \quad (2)$$

2.3. Adsorption column study

The experimental arrangement consists of a glass column of 0.2 dm inner diameter and 2.0 dm height. The column was equipped with a bottom filtration device to prevent the escape of fine resin beads during processing. The column was then loaded with 40 g (1.65 dm height) of PMR. The initial pH of the SEPRW having 500 mg L^{-1} of Cu(II) ions was adjusted to the pH range of 4–6 and allowed to pass through the column in batch recirculation and continuous mode using peristaltic pump. The concentration of Cu(II) ion gradually depleted in the reservoir. Experiments were conducted at different initial Cu(II) concentration (200, 300, 400 and 500 mg L^{-1}), different flow rates (0.005, 0.010, 0.015 L min^{-1}) and at different bed heights (0.55, 1.1 and 1.65 dm). Samples were collected at regular time intervals and were analysed for Cu(II) using AAS.

2.3.1. Column regeneration study

Adsorption process was carried out with initial concentration of 500 mg L^{-1} at the flow rate of 0.015 L min^{-1}, about 19.5 L of rinse water treated effectively and then the column exhausted. After exhaustion the rinse water present in the voids of resin beads was pumped out from the column. Desorption was carried out by passing 0.5 L of different molarities (0.5, 0.75, 1.0 and 1.5 M) of H_2SO_4 as eluant at constant flow rate (0.015 L min^{-1}) through the bed in batch recirculation mode. The concentration

of Cu(II) in the reservoir was monitored at different time intervals. It was observed that desorption cycle of the loaded resin took 50 min with 1.0 M H_2SO_4, after which further desorption was negligible. The desorbed column was washed with 1.0 L distilled water. The regenerated resin column performance was studied for second and more adsorption–desorption cycles.

2.4. Theoretical description

2.4.1. Modelling of batch ion exchange—isotherm studies

Ion-exchange isotherms are expressed in terms of relationship between the concentration of adsorbate in the liquid and the amount of adsorbate adsorbed by the unit mass of adsorbent at a constant temperature. Langmuir [33], Freundlich [34] isotherm models which are available in the literature were used to describe the equilibrium data.

2.4.2. Modelling of batch ion exchange—kinetic studies

The design of most equipment requires data on the amount of ions exchanged between solid phase and liquid phase in a given contact time. The ion-exchange kinetic studies describe the solute uptake rate which in turn governs residence time of an ion-exchange reaction. It is one of the important characteristics for defining the efficiency. The sorption kinetics of a sorbent depends mainly on the property of the sorbate. Hence, in this part of the present study, the kinetics for Cu(II) ions removal by PMR has been verified by pseudo-first [35] and second-order kinetics [36,37] to understand the behaviour of the resin.

2.4.3. Modelling of column ion exchange

The dynamic behaviour of the column can be predicted by various simple mathematical models. In this study, Adams–Bohart and Yoon–Nelson models were used to predict the performance of the column ion-exchange studies. The effect of flow rate on Cu(II) ions removal in column operation was investigated.

2.4.3.1. Adams–Bohart model. Bohart and Adams [38,39] established the fundamental equations that described the relationship between C/C_0 and t in a flowing system for the adsorption of chlorine on charcoal. The model proposed assumes that the adsorption rate is proportional to the residual capacity of the activated carbon and to the concentration of the sorbing species. The Adams–Bohart model provides a simple and comprehensive approach to running and evaluating sorption-column tests and valid to the range of conditions used. The model expression is given by:

$$\frac{C}{C_0} = \exp\left(K_{ab}C_0 t - K_{ab}N_0\frac{Z}{U_0}\right) \tag{3}$$

where K_{ab} is the kinetic constant (L mg^{-1} min^{-1}), U_0 is the superficial velocity calculated by dividing the flow rate by the column section area (cm min^{-1}) and Z is the bed depth of column (cm). C_0 is the influent concentration (mg L^{-1}); C is the effluent concentration (mg L^{-1}) at time t. Values describing the characteristic operational parameters of the column can be determined from the plot of $\ln C/C_0$ vs. t at a given bed height and flow rate.

2.4.3.2. Yoon–Nelson model. Yoon and Nelson [40] developed a model based on the assumption that the rate of decrease in the probability of adsorption of adsorbate molecule is proportional to the probability of the adsorbate adsorption and the adsorbate breakthrough on the adsorbent. The linearized Yoon–Nelson model for a single component system is expressed as:

$$\frac{C}{C_0 - C} = \exp(k_{YN}t - \tau k_{YN}) \tag{4}$$

where k_{YN} (min^{-1}) is the rate velocity constant, τ (min) is the time required for 50% adsorbate breakthrough. From a linear plot of $\ln[C/(C_0 - C)]$ against sampling time (t), values of k_{YN} and τ were determined from the intercept and slope of the plot $\ln(C/C_0 - C)$ vs. t.

2.4.3.3. BDST model. The BDST model is based on physically measuring the capacity of the bed at different breakthrough values. The BDST model works well and provides useful modelling equations for the changes of system parameters [41]. BDST column model is the simplest model which gives the useful information about the relationship between bed height (Z) and service time (t) of a column.

A modified form of the equation is given below [42]:

$$t = \frac{N_0 Z}{C_0 v} - \frac{1}{K_a C_0}\ln\left(\frac{C_0}{C_b} - 1\right) \tag{5}$$

where C_b is the breakthrough metal ion concentration (mg L^{-1}); N_0 the sorption capacity of bed per unit volume; v the linear velocity (cm h^{-1}) and K_a the rate constant (mg^{-1} h^{-1}).

$$Z = \frac{\upsilon}{K_a N_0} \ln\left(\frac{C_0}{C_b} - 1\right) \quad (6)$$

A simplified form of the BDST model is: $t = aZ + (-b)$.

where,

$$a = \frac{N_0}{C_0 F} \qquad b = -\frac{1}{K_a C_0} \ln\left(\frac{C_0}{C_t} - 1\right)$$

3. Results and discussion

3.1. Results of characterization

3.1.1. SEM–EDX analysis

The SEM equipped with EDX was used to analyse the components and morphology of cationic exchange resin surface. SEM–EDX analysis was done for UMR and PMR to understand the morphological changes and elemental changes. Fig. 2(a) and (b) shows that the surface morphology of the resin changed after PEI modification. The very smooth surface of UMR can be observed in Fig. 2(a) when compared to the agglomerated surface of PMR resin (Fig. 2(b)). The attachment of PEI on resin surface was confirmed by the SEM analysis. EDX results of UMR and PMR prove that the amount of carbon was increased by the impregnation of PEI. Through EDX analysis we could tell that the raw ion-exchange resin mainly comprises carbon, oxygen along with high content of silica. The peaks corresponding to carbon, oxygen, sulphur and silica were recorded in the EDX spectrum. These are all the elements present in the ion-exchange resin as main constituents. Through EDX analysis (Fig. 2), peaks of carbon increased gently in the PMR sample along with all other components identified in control ion-exchange resin sample. This confirms the addition of PEI in the resin matrix.

3.1.2. FTIR analysis

FTIR was used for functional group analysis of the resins, before and after PEI modification. The FTIR Spectra of UMR (a), PMR (b), is shown in Fig. 3. The spectrum of the pure ion-exchange resin is complex (Fig. 3(a)) due to the numerous functional groups. FTIR peaks prediction is given in Table 2. The peaks at 3,453, 2,924, 2,179, 1,643, 1,203 and 1,039 cm^{-1} were observed in the original resin. The broad and strong band at 3,453 cm^{-1} may be due to the overlapping of OH and N–H stretching. The strong peak at 1,643 cm^{-1} was assigned to secondary amine, N–H bending vibration. The peak at 2,924 cm^{-1} was attributed to CH stretching of CH_2 group [43]. The presence of C–N (aliphatic amines) was verified by the bands ranging from 1,020 to 1,250 cm^{-1}. After PEI cross linking, the spectrum exhibits some changes (Fig. 3(b)). The broad overlapping peak shifted to 3,467 cm^{-1} because a large number of amine groups in PEI were introduced into the resin matrix. Imine group introduction was confirmed by the characteristics broad peak at 1,638 cm^{-1} [44].

3.2. Effect of pH

To study the effect of pH on the removal efficiency of Cu(II) ions constant PMR resin dosage (1 g L^{-1}) was added to 0.1 L SEPRW which has 200 mg L^{-1} of Cu(II) ions and agitated for 1 h at 150 rpm.

The effect of pH on the removal efficiency of Cu (II) ions by PMR and its comparison with UMR performance is shown in Fig. 4(a). For unmodified ion-exchange resin, the Cu(II) uptake increased gradually as the pH increased from 2 and reached the maximum at pH 5–6 with the adsorption capacity of 164.3 mg g^{-1} whereas PMR shows maximum Cu(II) uptake of 200 mg g^{-1} at the same pH range. From pH 5 to 6 the adsorption capacity was found almost constant. In both instances, the adsorption as a function of solution pH showed a similar profile; the adsorption capacity increased sharply over the pH range from 2 to 5 after that a plateau was observed.

It is well known that solution pH is an important parameter affecting sorption of metal ions on adsorbents as it not only affects metal species in solution, but also influences the surface properties of the adsorbents [45,46]. As the protonation of sulphonic group in UMR and amine group in PMR occurs, the surface should be positively charged at pH below 5.0. Therefore, the electrostatic interactions between the resin and the metal ions of interest to be adsorbed were repulsive. Fewer uptakes at low pH values indicated that the hydrogen ion competition and hydrophobic behaviour of sorbate [47]. At alkaline pH range, the removal efficiency by both the resins decreases, whereas the metal ions get precipitated due to the formation of metal hydroxides. The OH^- ions available in the solution reacted with Cu(II) ions and formed $Cu(OH)_2$ precipitate [48]. Therefore, for better removal of Cu(II) ions the optimum pH range was selected as 5–6.

3.3. Effect of agitation time

The effect of agitation time on metal removal was studied by keeping other variables (pH 5 to 6 and

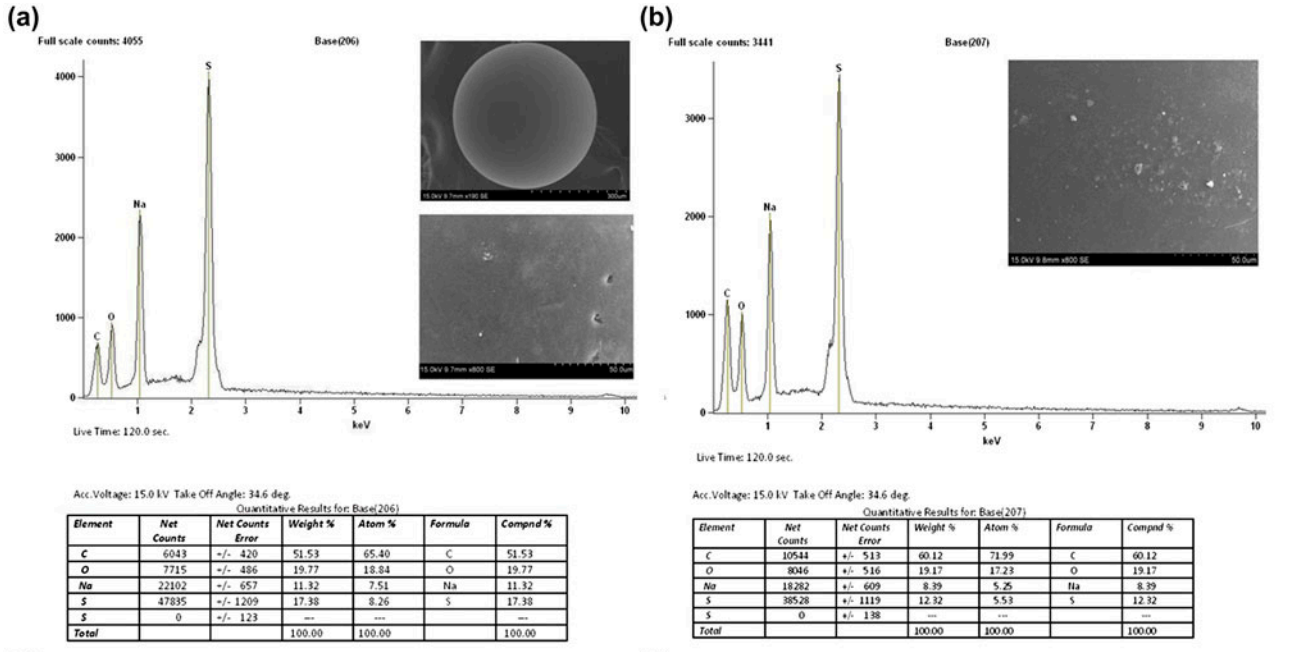

Acc.Voltage: 15.0 kV Take Off Angle: 34.6 deg.
Quantitative Results for: Base(206)

Element	Net Counts	Net Counts Error	Weight %	Atom %	Formula	Compnd %
C	6043	+/- 420	51.53	65.40	C	51.53
O	7715	+/- 486	19.77	18.84	O	19.77
Na	22102	+/- 657	11.32	7.51	Na	11.32
S	47835	+/- 1209	17.38	8.26	S	17.38
S	0	+/- 123	---	---		---
Total			100.00	100.00		100.00

Acc.Voltage: 15.0 kV Take Off Angle: 34.6 deg.
Quantitative Results for: Base(207)

Element	Net Counts	Net Counts Error	Weight %	Atom %	Formula	Compnd %
C	10544	+/- 513	60.12	71.99	C	60.12
O	8046	+/- 516	19.17	17.23	O	19.17
Na	18282	+/- 609	8.39	5.25	Na	8.39
S	38528	+/- 1119	12.32	5.53	S	12.32
S	0	+/- 138	---	---		---
Total			100.00	100.00		100.00

Acc.Voltage: 15.0 kV Take Off Angle: 34.6 deg.
Quantitative Results for: Base(208)

Element	Net Counts	Net Counts Error	Weight %	Atom %	Formula	Compnd %
C	5702	+/- 414	49.44	65.90	C	49.44
O	8609	+/- 504	23.45	23.46	O	23.45
S	37619	+/- 1050	15.40	7.69	S	15.40
S	0	0	---	---		---
Cu	3408	+/- 462	11.72	2.95	Cu	11.72
Cu	8135	+/- 579	---	---		---
Total			100.00	100.00		100.00

Acc.Voltage: 15.0 kV Take Off Angle: 34.6 deg.
Quantitative Results for: Base(209)

Element	Net Counts	Net Counts Error	Weight %	Atom %	Formula	Compnd %
C	7062	+/- 468	47.73	65.13	C	47.73
O	10054	+/- 567	20.82	22.89	O	20.82
Na	3918	+/- 693	1.88	2.01	Na	1.88
S	32559	+/- 1164	4.04	7.03	S	4.04
S	0	+/- 117	---	---		---
Ca	273	+/- 189	0.13	0.05	Ca	0.13
Ca	0	+/- 516	---	---		---
Cu	4935	+/- 345	25.39	2.88	Cu	25.39
Cu	12682	+/- 678	---	---		---
Total			100.00	100.00		100.00

Fig. 2. SEM–EDX analysis of (a) UMR, (b) PMR, (c) Cu(II) adsorbed UMR and (d) Cu(II) adsorbed PMR.

resin dosage as 1 g L^{-1}) as constant. Fig. 4(b) shows the effect of contact time on metal ions removal. Cu(II) ions removal efficiency increases rapidly with increase in time from 1 to 15 min later that it increased slowly and attained a maximum at 50 min for UMR, 20 min for PMR. The optimum contact time for Cu(II) ions removal by PMR was observed as 20 min (Fig. 4(b)) which is about 50% less than that of contact time taken by UMR. This study proves that, to get maximum Cu(II) ion uptake the PMR takes comparatively shorter time than the UMR.

3.4. Effect of resin dosage

The effect of resin dosage on Cu(II) ion removal was studied by varying the amount of PMR from

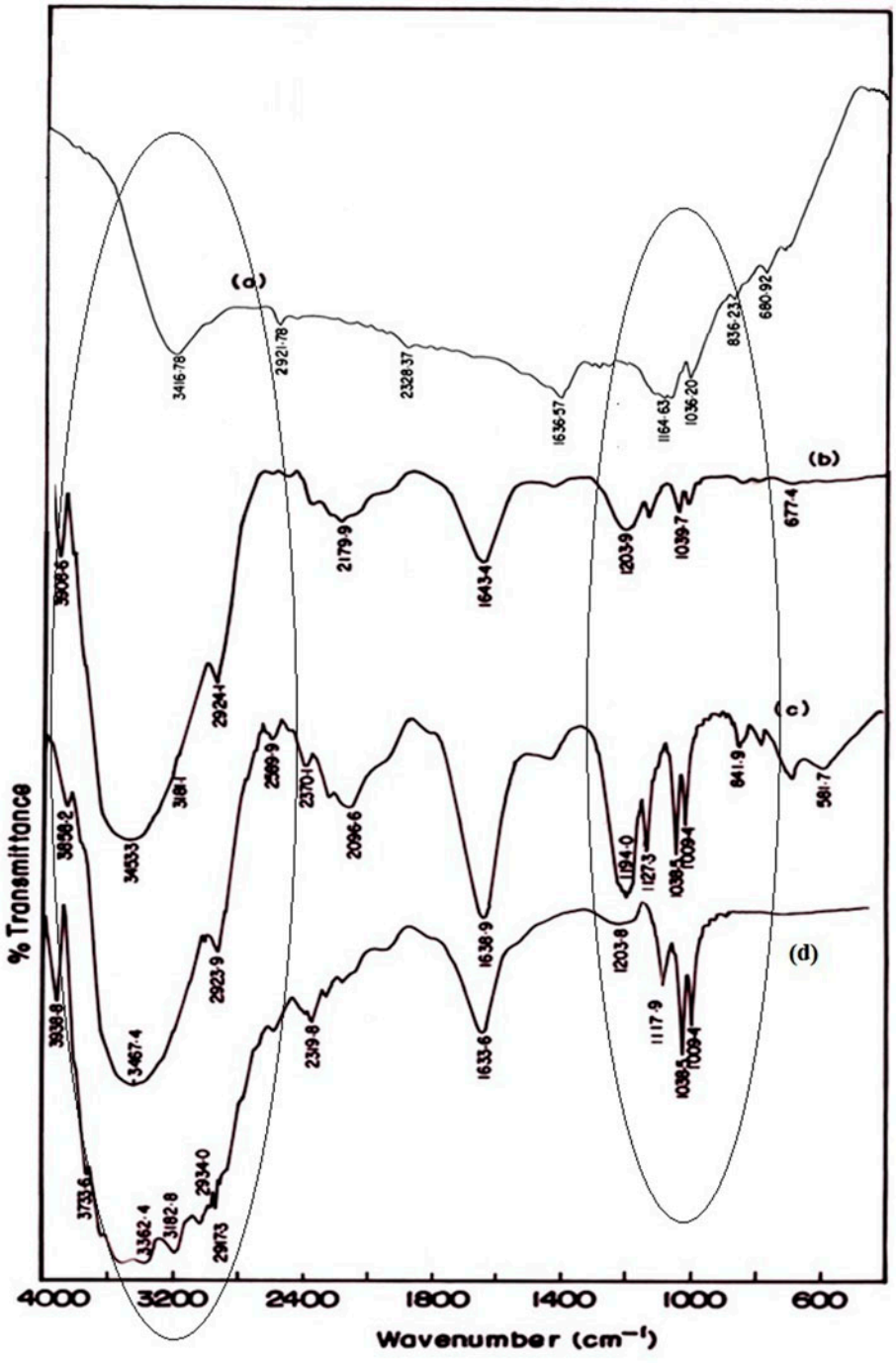

Fig. 3. FTIR spectra analysis (a) UMR, (b) PMR, (c) Cu(II) adsorbed UMR and (d) Cu(II) adsorbed PMR.

0.125 to 2.5 g for one litre of SEPRW. For this, the concentration of the Cu(II) ion (200 mg L^{-1}), solution pH (5–6), contact time (20 min) and the agitation speed (150 rpm) were kept constant. Fig. 4(c) shows the effect of resin dosage on the removal efficiency of Cu(II) ions by PMR. The percentage removal of metal ions increases sharply with increase in resin dosage and attained maximum of 99.9% at 0.5 g L^{-1}. There was no remarkable change in percentage removal with further increase in dosage. When the adsorbent dose increases, greater surface area or an adsorption site was provided for adsorption [49], which increases the

Table 2
Prediction of FTIR peaks

Frequency (cm^{-1})	Functional groups
3,453–3,362	Aromatic primary amine
2,924–2,917	C–H stretching vibration
2,179–2,096	C≡C vibration
2,589	OH stretching
2,179–2,096	C=C vibration
1,643–1,633	Secondary amine, NH bend
1,190–1,203	Secondary amine C–N stretching
1,039–1,127	C–N stretch aliphatic amines
1,009	C–O bond stretch

percentage removal gradually and attains the maximum. Hence, for further experiments resin dosage will be fixed as 0.5 g L^{-1}.

This study proved that the amount of PMR resin dosage required to remove 200 mg L^{-1} of Cu(II) has been reduced to half the amount utilized by UMR. The reason behind is that the presence of imine group in the PMR offered both ion exchange and chelation for the removal of Cu(II) ion.

3.5. Effect of initial concentration of Cu(II)

Cu(II) ions uptake with respect to increase of initial concentration in the SEPRW samples was studied by varying the concentration from 100 to 500 mg L^{-1} for the constant dosage of 1 g L^{-1} of ion-exchange resin. UMR showed increased metal uptake from 100 to 200 mg L^{-1}, after that the profile was unaltered with further increase of initial Cu(II) concentration. The rate of percentage removal of metal ions was higher in the

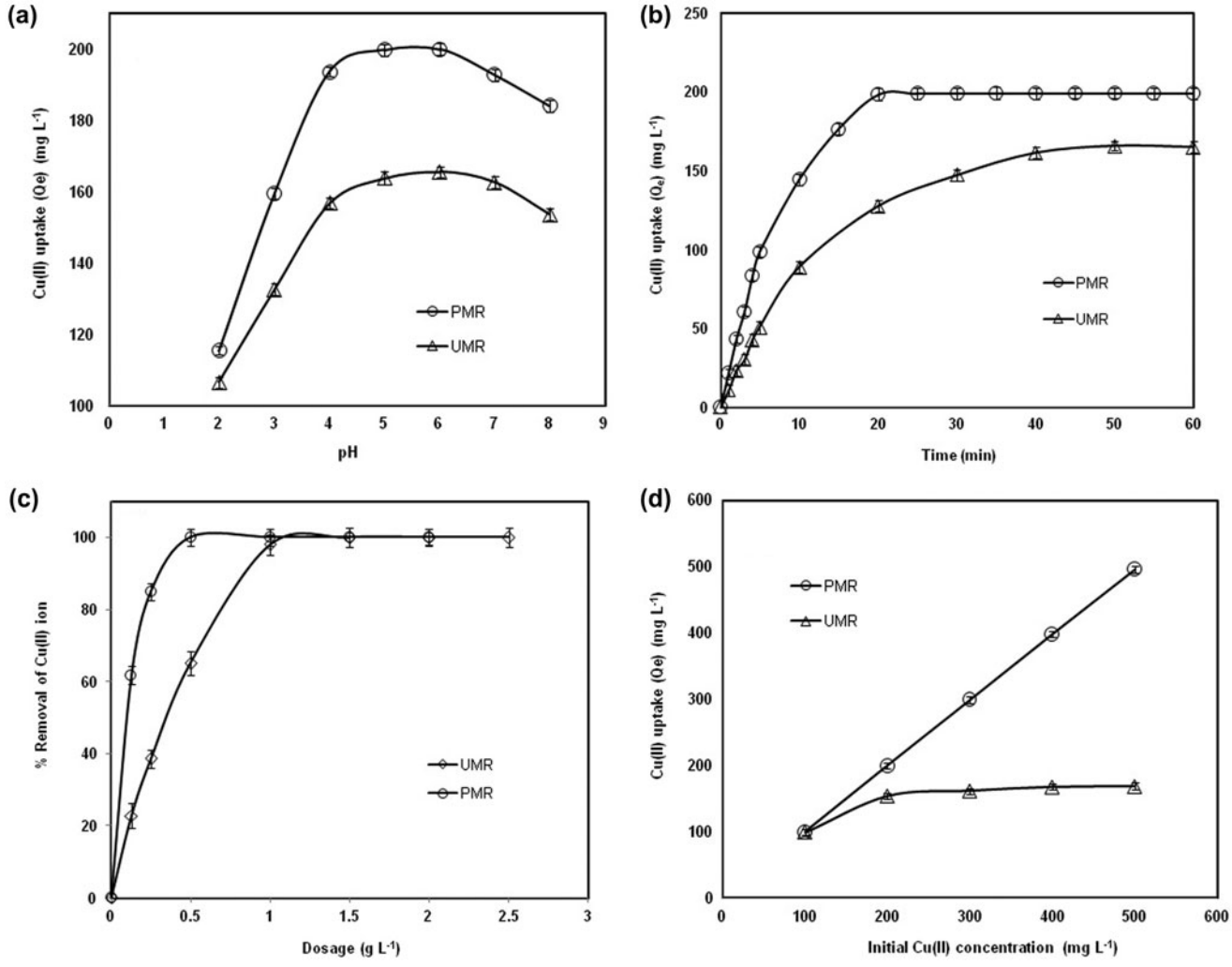

Fig. 4. Effect of experimental parameters on removal efficiency of Cu(II) by UMR and PMR. (a) Effect of pH, (b) effect of contact time, (c) effect of dose and (d) effect of initial concentration of Cu(II).

beginning due to the availability of larger surface area for adsorption. Adsorbed material formed a thick layer around the resin surface at once, then the capacity of the adsorbent got exhausted and further uptake rate was controlled by the rate of sorbate is transported from the exterior to the interior sites of the adsorbent.

Whereas the PMR showed the sharp increase in Cu(II) ion uptake with the increase of initial concentration of Cu(II) from 100 to 500 mg L^{-1} (Fig. 4(d)). This study reveals that the PMR provides additional space for freshly coming Cu(II) ions. This may due to the presence of long polymeric PEI matrix present in the resin which acts as a strong chelating agent for Cu (II) ions as well as it provides number of branched adsorption sites to the upcoming Cu(II) ions.

3.6. Effect of co-ions

The effect of two co-ions such as Ni(II) and Zn(II) ion on Cu(II) ion removal by PMR was studied with co-ion concentration of 250 mg L^{-1} and keeping the other variables as constant and the behaviour was compared with UMR. Fig. 5(a) and (b) shows the effect of co-ions Ni(II), Zn(II) on Cu(II) removal by both UMR and PMR. For UMR the rate of Cu(II) uptake was decreased by the presence of competing ions in the following order Zn(II) > Ni(II) ion. Whereas the Cu(II) metal ion uptake by PMR was not affected by the presence of Zn(II), Ni(II) (Fig. 5(b)). This may be because the sorbent showed more chelating property towards Cu(II) ions instead of other ions.

Moreover, the separation factor (α) played an important role in the selective removal of metal ions of interest. The α (Cu^{2+}–Ni^{2+}) and α (Cu^{2+}–Zn^{2+}) have been calculated by the quotient of the equivalent ionic fraction ratios, X_i, of two cations was studied. It was calculated from the following equation where the over bars indicate values within resin:

$$\alpha\ (Cu^{2+} - Ni^{2+}) = \frac{X_{Ni^{2+}} \times \overline{X_{Cu^{2+}}}}{X_{Cu^{2+}} \times \overline{X_{Ni^{2+}}}},$$

$$\alpha(Cu^{2+} - Zn^{2+}) = \frac{X_{Zn^{2+}} \times \overline{X_{Cu^{2+}}}}{X_{Cu^{2+}} \times \overline{X_{Zn^{2+}}}}$$

The separation factor obtained by this calculation was $\alpha(Cu^{2+}$–$Ni^{2+}) = 8.53$, $\alpha(Cu^{2+}$–$Zn^{2+}) = 9.78$. This separation factor played an important role in the selective ion exchange of Cu(II) ions by PMR. The α value greater than unity showed that Cu(II) ions got adsorbed predominantly than Ni(II) and Zn(II) ions [50].

Thus, the effect of co-ions proved that PEI modified Ceralite IR 120 has more capability to remove Cu (II) ions even in presence of common competing cations. This study reveals that the PMR can be applicable to the industrial effluent treatment processes also.

3.7. Effect of concentration of chelating agent EDTA

The effect of chelating agent (EDTA) on the performance of PMR should be studied to know the industrial application of PMR. EDTA is added to the plating bath to increase the solubility of metal ions by forming strong complexes. In addition to metal ions, an electroplating industrial effluent also contains certain concentrations of strong chelating agents like EDTA [51]. This chelating agent formed a stable complex with the Cu(II) ion in treatment processes. Investigation of such effect on metal ion removal was important in industrial point of view. A study was conducted by varying EDTA concentration in the rinse water from 50 to 250 mg L^{-1}. In the case of UMR increasing concentration of EDTA in the solution caused very tremendous decrease in copper removal (Fig. 5(b)). Nevertheless, Cu(II) ion uptake was not affected while treating the EDTA-rinse water with PMR ion-exchange resin, because the PEI itself is a strong chelating agent that has more attraction towards Cu (II) ions than EDTA.

3.8. Application of isotherm models

The maximum adsorption capacity of the PMR for Cu(II) ions was investigated over a range of metal concentrations of SEPRW from 50 to 250 mg L^{-1}. Fig. 6(a) presents a plot of the equilibrium adsorption amount (q_e, mg g^{-1}) vs. the equilibrium metal concentration in the solution (C_e, mg L^{-1}). Equilibrium data were fitted using the Langmuir and Freundlich adsorption isotherm. The Langmuir model served to estimate the maximum metal uptake values which could not be reached in the experiments. The constants evaluated are summarized in Table 3. A higher value of Q_{max} obtained from Langmuir model indicated the desirable affinity between the adsorbent and adsorbate molecules [52].

The Freundlich constant K_1, which denotes the binding capacity, was observed maximum for Cu(II) ions at optimum experimental conditions. The value of n obtained from Freundlich isotherm was >1 showed favourable nature of adsorption [52].

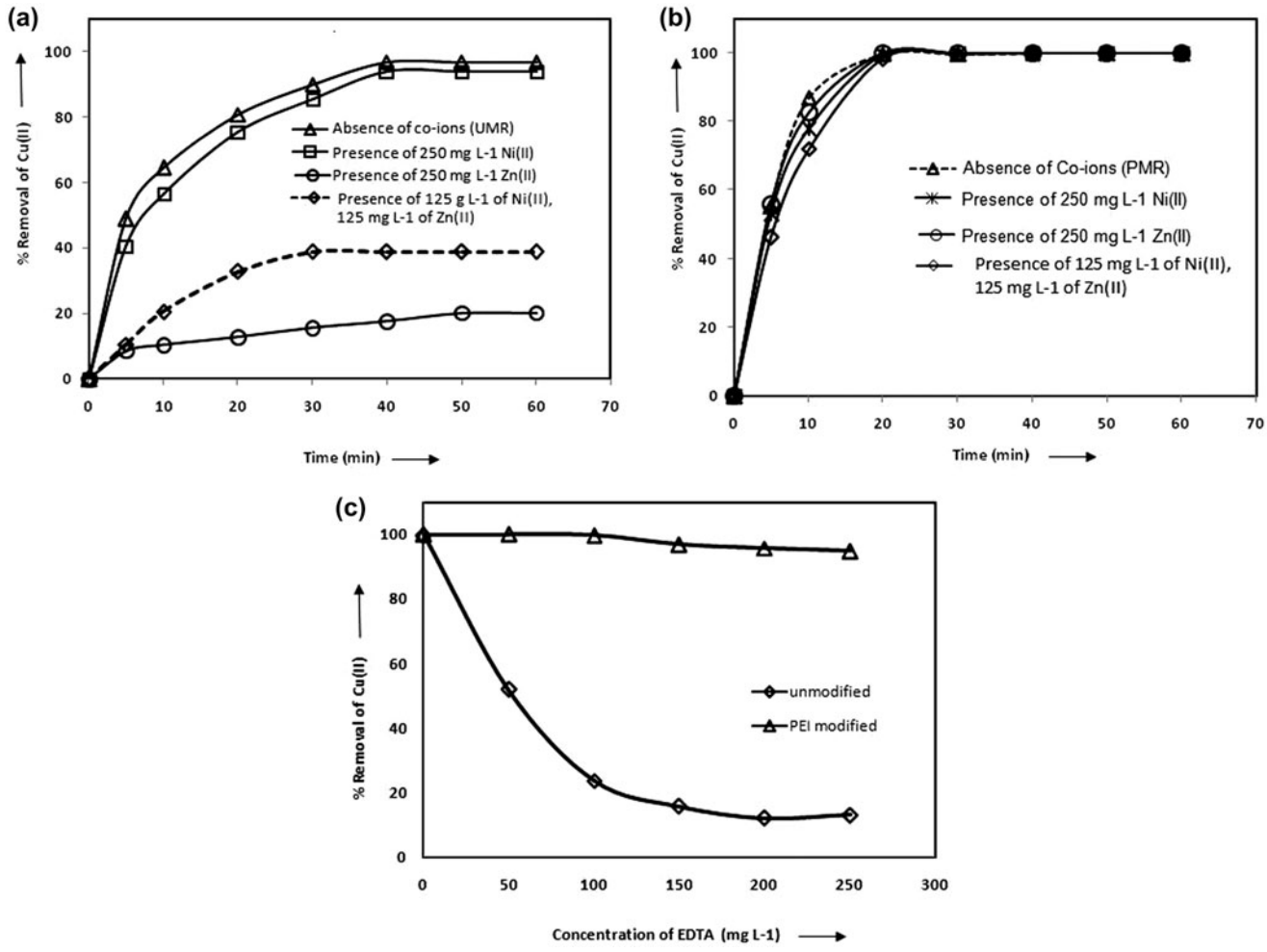

Fig. 5. (a) Effect of co-ions on Cu(II) removal by UMR, (b) effect of co-ions on Cu(II) removal by PMR and (c) effect of chelating agent EDTA on metal removal.

3.9. Application of kinetic models

In order to understand the kinetics of Cu(II) ions removal by PMR, pseudo-first-order and second-order models were fitted with experimental data that was obtained from batch experiments with the different initial metal ion concentrations and it is shown in Fig. 6(b). The rate constants, $q_{e(cal)}$ and correlation coefficients were calculated and summarized in Table 4. It revealed that the correlation coefficient of both first-order and second-order kinetic model is 0.99. Likewise, the theoretical ($q_{e(cal)}$) values calculated using both kinetic models were in good agreement with the experimental equilibrium uptake values ($q_{e(exp)}$). This shows that kinetics of Cu(II) ions removal by PMR is better described with pseudo-first-order and pseudo-second-order [36,37] indicating that the rate limiting steps was both physical and chemical adsorption process between metal ion and resin.

3.10. Results of column experiments

3.10.1. Effect of concentration—batch recirculation

The sorption performance of PMR Ceralite IR 120 was examined at different inlet Cu(II) concentrations of 300 to 500 mg L^{-1} at the flow rate of 0.005 L min^{-1}, 1.65 dm bed height. The trend of depletion of Cu(II) concentration in the reservoir is shown in Fig. 7(a). The time taken for 300 mg L^{-1} of Cu(II) is larger when compared to 500 mg L^{-1}, since the lower concentration gradient caused a slower transport due to decreased diffusion coefficient at lower concentration [53].

At the highest Cu(II) concentration (500 mg L^{-1}) the resin bed attracts the metal ions quickly due to concentration gradient. Thus high driving force due to high Cu(II) concentration resulted in better column performance.

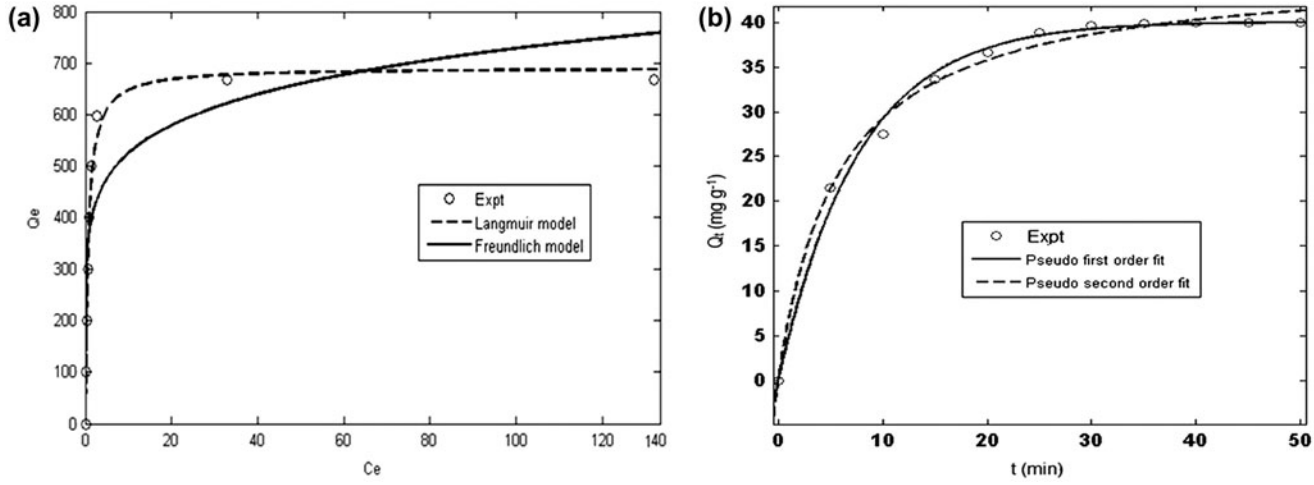

Fig. 6. Langmuir and Freundlich isotherm fit for the removal of Cu(II) by (a) PMR and (b) pseudo-first-order and second-order kinetics fit of PMR for Cu(II) removal.

Table 3
Adsorption isotherm parameters for Cu(II) removal by PMR and UMR comparison

Isotherm model	Constants	Unmodified resin (UMR)	PEI modified resin (PMR)
Langmuir	Q_{max} (mg g^{-1})	164.4	667.5
	b_1 (L g^{-1})	0.678	1.50
	R^2	0.9717	0.996
Freundlich	K_1 (L g^{-1})	78.53	381.8
	n	5.442	0.536
	R^2	0.8691	0.983

Table 4
Comparison of adsorption rate constants for the pseudo-first and second-order reaction kinetics of removal of Cu(II) ions by PMR

		Pseudo-first-order			Pseudo-second-order		
Metal ion	$q_{e(exp)}$ (mg g^{-1})	k_f (min^{-1})	$q_{e(cal)}$ (mg g^{-1})	R^2	k_S (g mg^{-1} min^{-1})	$q_{e(cal)}$ (mg g^{-1})	R^2
Copper	39.66	0.1304	40.06	0.994	0.0038	46.05	0.9858

3.10.2. Effect of flow rate—batch recirculation

The effect of flow rate on the adsorption of Cu(II) ions was studied in batch recirculation mode by varying the flow rates from 0.005 to 0.015 L min^{-1}, at fixed bed height (0.55 dm), pH (5.0) and at fixed inlet concentration of 500 mg L^{-1}. The depletion of Cu(II) concentration in the reservoir with time at different flow rate is shown in Fig. 7(b). In general, the increase of treatment time decreased the value of C/C_0 and reached the minimum of zero at particular time. Lower flow rate of 0.005 L min^{-1} took longer time (10 h) to reduce the Cu(II) content in the rinse water to permissible discharge limit of 2 mg L^{-1}. While the higher flow rate studied treats the rinse water in shorter period (2.5 h) with the removal efficiency of 99.0%. This behaviour may be due to insufficient input of Cu(II) for the resin column at lower flow rate. For further experiments the flow rate was fixed at 0.015 L min^{-1}.

3.10.3. Effect of bed height—continuous

In the column continuous experiments, the bed height was varied from 0.55 to 1.65 dm. In order to

yield different bed heights, 10, 20 and 40 g of PMR were added in the column to produce 0.55, 1.10 and 1.65 dm, respectively. The inlet Cu(II) concentration (500 mg L^{-1}) and the flow rate (0.015 L min^{-1}) were kept constant. As shown in Fig. 7(c), both the breakthrough and exhaustion time increased with increasing bed height. The reason behind increase in the uptake capacity of Cu(II) ions as bed height increases is availability of more binding sites for sorption, which also resulted in a broadened mass transfer zone.

3.11. Application of ion-exchange column models

3.11.1. Adams–Bohart model

The model developed by Bohart and Adams was applied to investigate the initial part of the breakthrough behaviour of PMR resin studied. This approach was focused on the estimation of characteristic parameters, such as maximum adsorption capacity (N_0) and kinetic constant (K_{ab}). After applying Eq. (3) to the experimental data, the parameters were obtained for the relative concentration region (50% breakthrough). The values of K_{ab} (the kinetic constant) and N_0 (the maximum amount of metal exchanged) are determined from plots of $\ln(C/C_0)$ against t at different bed height and presented in Table 5. It was observed that both K_{ab} and N_0 increased with increased in bed height for a given flow rate. It is clear from Fig. 7(c) that there is a good agreement between the experimental and predicted breakthrough values, suggesting that the Adams–Bohart model will be valid for this concentration region.

3.11.2. Yoon–Nelson model

The Yoon and Nelson model is based on the assumption that the rate of decrease in the probability of adsorption for each sorbate molecule is proportional to the probability of sorbate sorption and to the probability of sorbate breakthrough. The Yoon and Nelson model is straightforward than the other models [54]. This model was applied according to Eq. (4) to describe the breakthrough behaviour of PMR Ceralite IR 120. The values of k_{YN} and τ were determined from $\ln[C/(C_0 - C)]$ against t plots at different bed heights (0.55, 1.1 and 1.65 dm) (Fig. 7(d)) and the values are listed in Table 5. The values for the kinetic constant (k_{YN}) have the same order of magnitude for all the three bed heights. It is expected that the value of τ increases with the increase of bed height, because the higher the resin surface the higher the saturation period. This is verified in the experimental assays described here. The theoretical curves are compared with the corresponding experimental data in Fig. 7(d) and it could be concluded that the experimental breakthrough curves were followed very closely by the Yoon–Nelson model, for all the bed heights tested.

3.11.3. BDST model

The simplicity of the BDST model is that it can predict the slope for any unknown bed height variation of the column with a known slope. The breakthrough time against the bed height is shown in Fig. 7(e).

The nature of the plot was very linear ($R^2 = 0.990$) indicating the validity of the BDST model for PMR resin towards Cu(II) ions removal. The slope and intercept value was calculated using straight line equation and used for the model parameter calculations. The parameters thus found are $N_0 = 277.95$ mg L^{-1}, $v = 0.051$ cm h^{-1}, $K_a = 0.0277$ mg^{-1} h^{-1}. The estimated parameter of the BDST model (N_0, the adsorption capacity; rate constant K_b; the linear velocity v) for Cu (II) ions removal by PMR system. These BDST model parameters can be useful in scaling up the process [55].

3.12. Comparison of breakeven point

An experimental study was carried out to determine the breakthrough point of the UMR and PMR in a column reactor. It is very important to study the operational capacity of the UMR and PMR. The same weight (40 g) of the UMR and PMR were packed in different glass columns, and the test solutions taken in different reservoir containing 500 mg L^{-1} of Cu(II) were made to run through the columns separately and continuously. Fig. 8(a) shows the comparison of break point of the columns packed with unmodified, PMR ion-exchange resin. The break-through curve showed that at the outlet the concentration of Cu(II) is zero up to a certain point of discharge of volume collected and then the concentration of Cu(II) ion increased and reached its initial value as if the bed has attained saturation.

The break point for the PMR column is quite higher (19.5 L) than that of the unmodified (4.5 L) one. Therefore, the break-even analysis proved the PEI modification of Ceralite IR 120 increased the capacity of the parent considerably.

3.13. Regeneration, recovery

3.13.1. Batch mode

An amount of 0.1 g of Cu(II) saturated PMR was immersed in 0.1 L of different acid solutions (0.5 M

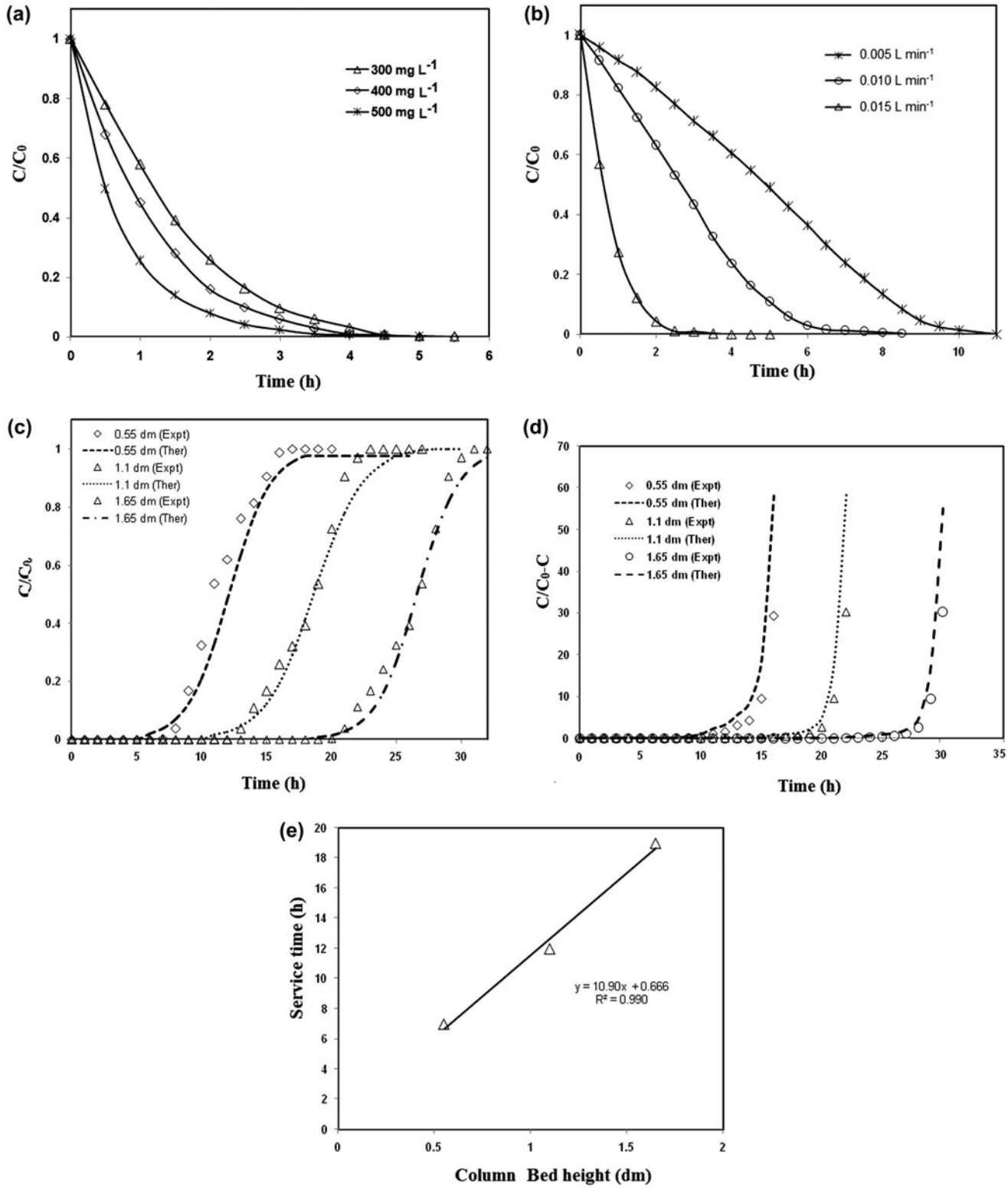

Fig. 7. Concentration–time behaviour of recirculating ion-exchange adsorption column (a) at constant bed height = 1.65 dm, flow rate = 0.005 L min^{-1} at different initial Cu(II) concentration, (b) at constant Cu(II) concentration = 500 mg L^{-1}, at different flow rate, (c) Adams–Bohart experimental and predicted breakthrough curves of Cu(II) adsorption by PEI modified resin column at different flow rates at constant bed height of 16.5 cm, (d) Yoon and Nelson model breakthrough curves at different bed heights, constant flow rate and (e) BDST model fit for PMR.

Table 5
Comparison of continuous column model constants

Bed height (dm)	wt. (g)	Break point (h)	Adam–Bohart model			Yoon–Nelson model		
			K_{ab}	N_0 (mg L^{-1})	R^2	k_{YN} (min^{-1})	t (min)	R^2
0.55	10	7	0.000212	52,735.6	0.944	0.724	11.51	0.964
1.10	20	12	0.000502	119,124.6	0.958	0.650	17.88	0.954
1.65	40	19	0.000562	227,723.7	0.963	0.610	27.57	0.954

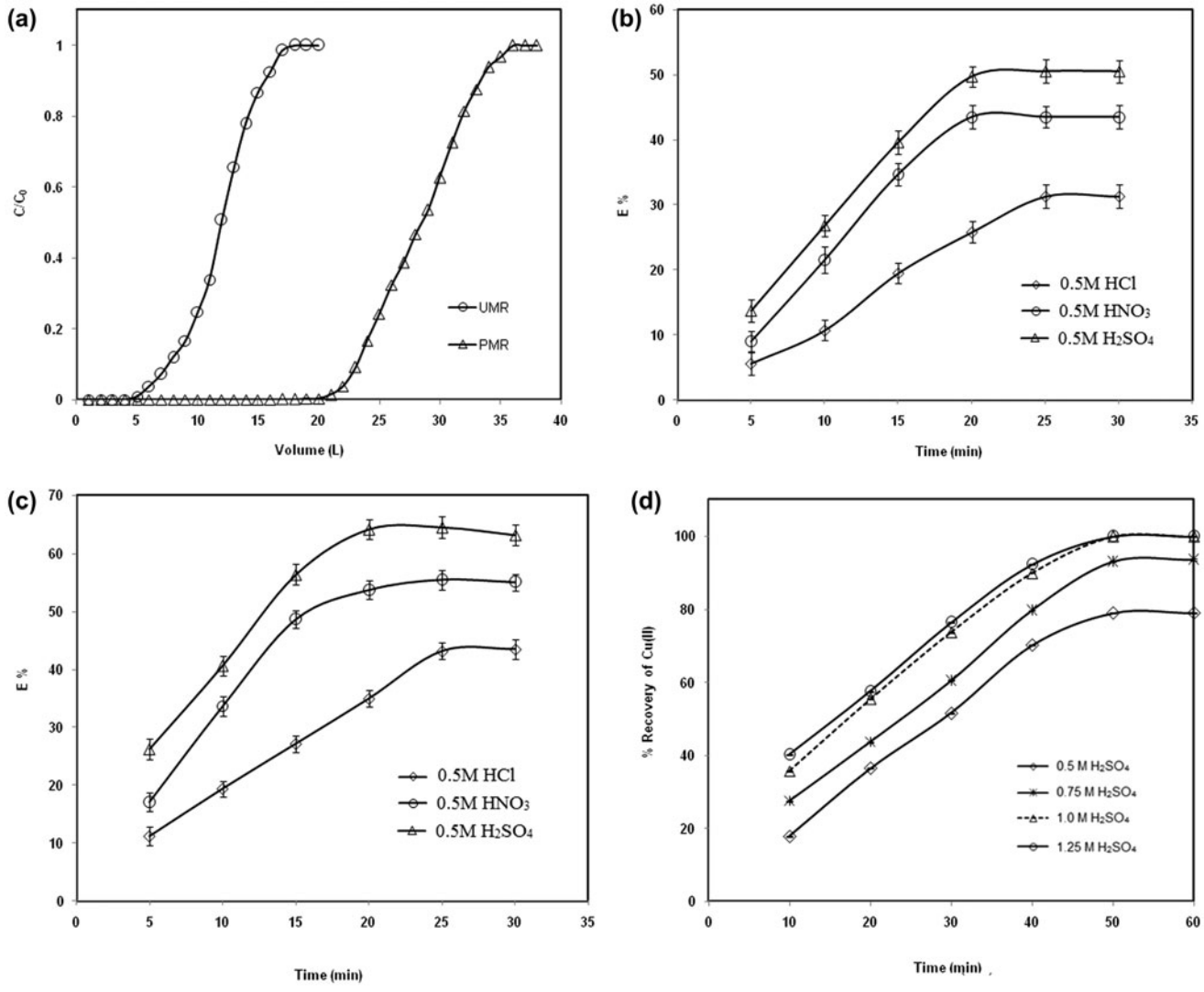

Fig. 8. (a) Comparison of breakeven point of the UMR and PMR, (b) desorption of copper loaded UMR by different acids as eluant, (c) desorption of copper loaded PMR by different acids as eluant and (d) desorption of copper loaded resin column with different molarity of sulphuric acid as eluant at a constant flow rate of 0.015 L min^{-1}.

HNO_3, 0.5 M HCl and 0.5 M H_2SO_4), and the systems were agitated for 2 h, then filtered. The filtrate was analysed for copper by AAS and the per cent of elution (E %) was calculated and plotted in Fig. 8(b) and (c) for UMR and PMR. It was observed that the 0.5 M H_2SO_4 solution eluted maximum percentage of Cu(II) for both the resins (UMR and PMR) investigated. The percentage of elution of Cu(II) ions from PMR was

found to be higher with H_2SO_4. The percentage elution from PMR was found to be higher than the UMR with H_2SO_4 because each molecule of H_2SO_4 provides 2 hydrogen ions and the H_2SO_4 was selected as suitable eluant.

3.13.2. Column mode

One litre SEPRW having 500 mg L^{-1} of Cu(II) was recirculated through 16.5 cm resin column (40 g) until all the Cu(II) ions removed. Adsorbed Cu(II) ions were desorbed by different molarity of H_2SO_4 (0.5, 0.75, 1.0 and 1.25 M) in smallest possible volume (0.2 L) of the reservoir in batch recirculation mode. The results of desorption process is shown in Fig. 8(d). As the concentration of H_2SO_4 increased the percentage of elution also increased and with a concentration of 1.25 M maximum elution was achieved.

3.14. FTIR analysis

The FTIR Spectra of UMR (a), PMR (b), Cu(II) exchanged UMR (c) and Cu(II) exchanged PMR (d) are shown in Fig. 3. The spectrum of the pristine ion-exchange resin is complex due to the numerous functional groups. The peaks at 3,453, 2,924, 2,179, 1,643, 1,203 and 1,039 cm^{-1} are observed in the original resin. The peaks interpretation is given in Table 2. The broad and strong band at 3,453 cm^{-1} may be due to the overlapping of OH and N–H stretching. The string peak at 1,643 cm^{-1} assigned to secondary amine, N–H bending vibration. The peak at 2,924 cm^{-1} is attributed to CH stretching. The presence of C–N (aliphatic amines) is verified by the bands ranging from 1,020 to 1,250 cm^{-1} [56]. For fresh ion-exchange resin the peaks observed at 1,164 cm^{-1} and 1,036 cm^{-1} corresponds to the functional sulphonic acid group (–SO_3H) and the other peak (836 cm^{-1}) corresponds to para-di-placed benzene. After PEI was cross linked with the resin, the spectrum exhibits some changes (Fig. 3). The broad overlapping peak shifts to 3,467 cm^{-1} because a large number of amine groups in PEI were introduced into the resin matrix. Imine group introduction was confirmed by the characteristics broad peak at 1,638 cm^{-1} [43].

The changes in the FTIR peaks of the UMR, PMR after copper uptake were noted from Fig. 3(c) and (d). The peak at 3,467 cm^{-1} attributed to N–H bending shifts to the lower peak at 3,362 cm^{-1} after copper uptake. Similarly, the characteristics peak of 1,194 cm^{-1} shifts to 1,117 cm^{-1}. The broad overlap region 3,467 cm^{-1} split into number of peaks showed that in PMR the N–H groups and C–N groups were the responsible for adsorption.

3.15. SEM–EDX analysis

SEM–EDX measurements were taken for UMR and PMR before and after adsorption of Cu(II) ions at 9.6 mm × 120 SE, 15.0 kV from 0 to 500 μm. After sorption, considerable changes in surface morphology of ion-exchange resins were observed. Surface protuberances decreased and thin layer of deposition was observed (Fig. 2(c) and (d)). Through EDX analysis peaks of the Cu(II) ions examined were observed in the sample along with all other components identified in control sample. In that the unmodified ion-exchange resin shows lower Cu(II) peak when compared to PMR ion-exchange resin.

4. Conclusions

PEI modified Ceralite IR 120 ion-exchange resin (PMR) have been used as adsorbent the removal of Cu(II) ions from SEPRW electroplating rinse water solutions at room temperature (35˚C). The following results were obtained. The PMR was found to be a better sorbent for the removal of Cu(II) ions from SEPRW than the UMR. The optimum time for maximum Cu(II) ions uptake was 20 min. The effective adsorbent dosage was found to be 0.5 g L^{-1} for Cu(II) which is half of the UMR amount required. The optimum pH range for effective metal removal was found to be pH 5–6. The isotherm studies fits well with Langmuir, Freundlich models. The maximum adsorption capacity (Q_{max}) was in the order: PMR > UMR. A SEM EDX analysis confirms the impregnation of PEI into the resin matrix and the improvement of uptake capacity of the Ceralite IR 120 by PEI modification. FTIR study confirms N–H and C–N groups of PMR were the main functional groups responsible for metal binding. Column studies fit well to Adam–Bohart, Yoon–Nelson and BDST models. In the continuous column process, break point obtained after the treatment of several litres (19.5 L) of rinse water for an inlet concentration of 500 mg L^{-1} of metal ions. Most of the copper metal sorbed in the resin was successfully eluted from the column by 1.0 M H_2SO_4. This treated rinse water could be reused in the rinsing tanks, and the resin regenerated at the end can be recycled in the subsequent treatment processes.

Acknowledgement

The author Meyyappan Revathi is grateful to University Grant Commission, India for the award of senior research fellowship.

Abbreviations

SEPRW	—	synthetic electroplating rinse water
PMR	—	PEI modified resin
UMR	—	unmodified resin

Nomenclature

C_0	—	initial Cu(II) concentration (mg L^{-1})
C_t	—	Cu(II) concentration at specific time (mg L^{-1})
Q_t	—	adsorption capacity at specific time t (mg g^{-1})
Q_{max}	—	maximum adsorption capacity (mg g^{-1})
b_1	—	Langmuir isotherm constant (L g^{-1})
K_l	—	capacity of adsorption (L g^{-1})
n	—	intensity of adsorption
C_0	—	influent Cu(II) concentration (mg L^{-1})
C	—	outlet Cu(II) concentration (mg L^{-1}) at time t
Q	—	flow rate (L min^{-1})
K_{ab}	—	Adams–Bohart kinetic constant (L mg^{-1} min^{-1})
U_0	—	Superficial velocity (cm min^{-1});
Z	—	BED depth of column (cm)
N_0	—	saturation concentration (mg L^{-1})
k_{YN}	—	the rate velocity constant (min^{-1})
τ	—	the time required for 50% adsorbate breakthrough (min)

References

[1] M.S. Holt, Sources of chemical contaminants and routes into the freshwater environment, Food Chem. Toxicol. 38(1) (2000) S21–S27.

[2] M. Ajmal, R.A.K. Rao, R. Ahmad, J. Ahmad, L.A.K. Rao, Removal and recovery of heavy metals from electroplating wastewater by using Kyanite as an adsorbent, J. Hazard. Mater. 87 (2001) 127–137.

[3] Y.S. Al-Degs, M.F. Tutunju, R.A. Shawabkeh, The feasibility of using diatomite and Mn–diatomite for remediation of Pb^{2+}, Cu^{2+}, and Cd^{2+} from water, Sep. Sci. Technol. 35 (2000) 2299–2310.

[4] P. Kaewsarn, Biosorption of copper(II) from aqueous solutions by pre-treated biomass of marine algae *Padina* sp., Chemosphere 47 (2002) 1081–1085.

[5] M.D. Machado, H.M.V.M. Soares, E.V. Soares, Removal of chromium, copper, and nickel from an electroplating effluent using a flocculent brewer's yeast strain of *Saccharomyces cerevisiae*, Water, Air, Soil Pollut. 212 (2010) 199–204.

[6] G. Yan, T. Viraraghavan, Heavy metal removal from aqueous solution by fungus *Mucor rouxii*, Water Res. 37 (2003) 4486–4496.

[7] O.I. Oboh, E.O. Aluyor, The removal of heavy metal ions from aqueous solutions using sour soup seeds as biosorbents, African J. Biotechnol. 7(24) (2008) 4508–4511.

[8] M.A. Hossain, H.H. Ngo, W.S. Guo, T.V. Nguyen, S. Vigneswaran, Performance of cabbage and cauliflower wastes for heavy metals removal, Desalin. Water Treat. 52 (2014) 844–860.

[9] F. Mohammed-Azizi, S. Dib, M. Boufatit, Removal of heavy metals from aqueous solutions by Algerian bentonite, Desalin. Water Treat. 51 (2013) 4447–4458.

[10] K. Vijayaraghavan, K. Palanivelu, M. Velan, Biosorption of copper(II) and cobalt(II) from aqueous solutions by crab shell particles, Bioresour. Technol. 97 (2006) 1411–1419.

[11] F. Calisir, F.R. Roman, L. Alamo, O. Perales, M.A. Arocha, S. Akman, Removal of Cu(II) from aqueous solutions by recycled tire rubber, Desalination 249 (2009) 515–518.

[12] S.S. Ahluwalia, D. Goyal, Removal of heavy metals by waste tea leaves from aqueous solution, Eng. Life Sci. 5(2) (2005) 158–162.

[13] E.-S.Z. El-Ashtoukhy, N.K. Amin, O. Abdelwahab, Removal of lead(II) and copper(II) from aqueous solution using pomegranate peel as a new adsorbent, Desalination 223 (2008) 162–173.

[14] Y.H. Chen, F. Li, Kinetic study on removal of copper (II) using goethite and hematite nano-photocatalysts, J. Colloid Interface Sci. 347(2) (2010) 277–281.

[15] W. Chouyyok, Y. Shin, J. Davidson, W.D. Samuels, N.H. LaFemina, R.D. Rutledge, G.E. Fryxell, Selective removal of copper(II) from natural waters by nanoporous sorbents functionalized with chelating diamines, Environ. Sci. Technol. 44(16) (2010) 6390–6395.

[16] M. Ozmen, K. Can, G. Arslan, A. Tor, Y. Cengeloglu, M. Ersoz, Adsorption of Cu(II) from aqueous solution by using modified Fe_3O_4 magnetic nanoparticles, Desalination 254 (2010) 162–169.

[17] W. Yantasee, C.L. Warner, T. Sangvanich, R.S. Addleman, T.G. Carter, R.J. Wiacek, G.E. Fryxell, C.T. Chalk, M.G. Warner, Removal of heavy metals from aqueous systems with thiol functionalized superparamagnetic nanoparticles, Environ. Sci. Technol. 41 (14) (2007) 5114–5119.

[18] X. Liu, Q. Hu, Z. Fang, X. Zhang, B. Zhang, Magnetic chitosan nanocomposites: A useful recyclable tool for heavy metal ion removal, Langmuir 25 (2009) 3–8.

[19] H.V. Tran, L.D. Tran, T.N. Nguyen, Preparation of chitosan/magnetite composite beads and their application for removal of Pb(II) and Ni(II) from aqueous solution, Mater. Sci. Eng.: C 30 (2010) 304–310.

[20] A.H. Elshazly, A.H. Konsowa, Removal of nickel ions from wastewater using a cation-exchange resin in a batch-stirred tank reactor, Desalination 158(1–3) (2003) 189–193.

[21] S. Rengaraj, J.W. Yeon, Y. Kim, Y. Jung, Y.K. Ha, W.H. Kim, Adsorption characteristics of Cu(II) onto ion exchange resins 252 and 1,500 H: Kinetics, isotherms and error analysis, J. Hazard. Mater. 143 (2007) 469–477.

[22] S. Verbych, N. Hilal, G. Sorokin, M. Leaper, Ion exchange extraction of heavy metal ions from wastewater, Sep. Sci. Technol. 39(9) (2004) 2031–2040.

[23] B. Alyuz, S. Veli, Kinetics and equilibrium studies for the removal of nickel and zinc from aqueous solutions by ion exchange resins, J. Hazard. Mater. 167 (2009) 1–3.

[24] D. Rabelo, E.C.D. Lima, A.C. Reis, Preparation of magnetite nanoparticles in mesoporous copolymer template, Nano Lett. 1(2) (2001) 105–108.

[25] T. Saitoh, F. Nakane, M. Hiraide, Preparation of trioctylamine-impregnated polystyrene–divinylbenzene porous resins for the collection of precious metals from water, React. Funct. Polym. 67(3) (2007) 247–252.

[26] Y. Chen, B. Pan, H. Li, W. Zhang, L. Lv, J. Wu, Selective removal of Cu(II) Ions by using cation-exchange resin-supported polyethyleneimine (PEI) nanoclusters, J. Hazard. Mater. 44 (2010) 3508 –3513.
[27] M. Amara, H. Kerdjoudj, Modification of the cation exchange resin properties by impregnation in poly-ethyleneimine solutions application to the separation of metallic ions, Talanta 60 (2003) 991–1001.
[28] M. Chanda, G.L. Rempel, Chromium(III) removal by poly(ethyleneimine) granular sorbents made by a new process of templated gel filling, React. Funct. Polym. 35 (1997) 197–207.
[29] M. Revathi, M. Saravanan, C. Ahmed Basha, M. Velan, Removal of copper, nickel, and zinc ions from electroplating rinse water, Clean—Soil, Air, Water 40 (2012) 66–79.
[30] R. Bahulekar, N.R. Ayyangar, S. Ponrathnam, Poly-ethyleneimine in immobilization of biocatalysts, Enzyme Microb. Technol. 13(11) (1991) 858–868.
[31] S. Deng, Y.P. Ting, Characterization of PEI-modified biomass and biosorption of Cu(II), Pb(II) and Ni(II), Water Res. 39 (2005) 2167–2177.
[32] M. Ghoul, M. Bacquet, M. Morcellet, Uptake of heavy metals from synthetic aqueous solutions using modified PEI-silica gels, Water Res. 37 (2003) 729–734.
[33] I. Langmuir, The adsorption of gases on plane surfaces of glass, mica and platinum, J. Am. Chem. Soc. 40(9) (1918) 1361–1403.
[34] H. Freundlich, Adsorption in solutions, J. Phys. Chem. 57 (1906) 384–470.
[35] S. Lagergren, About the theory of so called adsorption of soluble substances, Kungligu Svenska Vetenskap-sakademiens, Handlingar 24 (1898) 1–39.
[36] Y.S. Ho, G. McKay, The sorption of lead(II) ions on peat, Water Res. 33 (1999) 578–584.
[37] Y.S. Ho, G. McKay, The kinetics of sorption of divalent metal ions onto sphagnum moss peat, Water Res. 34 (2000) 735–742.
[38] Z. Aksu, F. Gönen, Biosorption of phenol by immobilized activated sludge in a continuous packed bed: Prediction of breakthrough curves, Process Biochem. 39 (2004) 599–613.
[39] R. Han, D. Ding, Y. Xu, W. Zou, Y. Wang, Y. Li, L. Zou, Use of rice husk for the adsorption of congo red from aqueous solution in column mode, Bioresour. Technol. 99 (2008) 2938–2946.
[40] Y.H. Yoon, J.H. Nelson, Application of gas adsorption kinetics I. A theoretical model for respirator cartridge service life, Am. Ind. Hyg. Assoc. J. 45 (1984) 509–516.
[41] D.C.K. Ko, J.F. Porter, G. McKay, Optimised correlations for the fixed bed adsorption of metal ions on bone char, Chem. Eng. Sci. 55 (2000) 5819–5829.
[42] J. Goel, K. Kadirvelu, C. Rajagopal, V.K. Garg, Removal of lead(II) by adsorption using treated granular activated carbon: Batch and column studies, J. Hazard. Mater. 125 (2005) 211–220.
[43] J. Coates, Interpretation of infrared spectra, a practical approach, in: R.A. Meyers (Ed.), Encyclopedia of Analytical Chemistry, John Wiley and Sons Ltd, Chichester, 2000, pp. 10815–20837.
[44] B. Volesky, S. Schiewer, Biosorption of metals, in: M. Flickinger, S.W. Drew (Eds.), Encyclopedia of Bioprocess Technology, Wiley, New York, NY, 1999, pp. 433–453.
[45] P.X. Sheng, Y.P. Ting, J.P. Chen, L. Hong, Sorption of lead, copper, cadmium, zinc, and nickel by marine algal biomass: Characterization of biosorptive capacity and investigation of mechanisms, J. Colloid Interface Sci. 275(1) (2004) 131–141.
[46] S.B. Deng, R.B. Bai, Removal of trivalent and hexavalent chromium with aminated polyacrylonitrile fibers: Performance and mechanisms, Water Res. 38(9) (2004) 2424–2432.
[47] S. Veli, B. Pekey, Removal of copper from aqueous solutions by ion exchange resins, Fresenius Environ. Bull. 13(1–3) (2004) 244–250.
[48] C.Y. Kao, K.S. Chou, Electroless copper plating onto printed lines of nanosized silver seeds, Electrochem. Solid-State Lett. 10(3) (2007) D32–D34.
[49] P. Sudamalla, S. Pichiah, M. Manickam, Responses of surface modeling and optimization of Brilliant Green adsorption by adsorbent prepared from *Citrus limetta* - peel, Desalin. Water Treat. 50 (2012) 367–375.
[50] A. Smara, R. Delimi, E. Chainet, J. Sandeaux, Removal of heavy metals from diluted mixtures by a hybrid ion-exchange/electrodialysis process, Sep. Purif. Technol. 57 (2007) 103–110.
[51] T.H. Madden, A.K. Datye, M. Fulton, Oxidation of Metal−EDTA complexes by TiO_2 photocatalysis, Environ. Sci. Technol. 31(12) (1997) 3475–3481.
[52] R.E. Treybal, Mass Transfer Operations, third ed., McGraw-Hill, New York, NY, 1980, pp. 527–529.
[53] Z. Aksu, S.S. Çağatay, F. Gönen, Continuous fixed bed biosorption of reactive dyes by dried *Rhizopus arrhizus:* Determination of column capacity, J. Hazard. Mater. 143(1–2) (2007) 362–371.
[54] C. Quintelas, B. Silva, H. Figueiredo, T. Tavares, Removal of organic compounds by a biofilm supported on GAC: Modelling of batch and column data, Biodegradation 21 (2010) 379–392.
[55] Z. Zulfadhly, M.D. Mashitah, S. Bhatia, Heavy metals removal in fixed-bed column by the macro fungus *Pycnoporus sanguineus*, Environ. Pollut. 112 (2001) 463–470.
[56] M. Thomas, H.H. Richardson, Two-dimensional FT-IR correlation analysis of the phase transitions in a liquid crystal, 4´-n-octyl-4-cyanobiphenyl (8CB), Vib. Spectro. 24 (2000) 137–146.